Analysis of the polarization on the bidirectional channel characteristics in an outdoor-to-indoor office scenario

I. Vin, D. P. Gaillot, P. Laly, J. M. Molina-Garcia-Pardo, M. Lienard and P. Degauque

***Abstract*—**This paper presents experimental results on the influence of the polarization on the outdoor-to-indoor channel characteristics and for a frequency range around 1.3 GHz. Virtual antenna arrays have been used both at the transmitting and the receiving sites. Path loss and delay spread are deduced from measurements carried out for different positions of the receiver, from indoor light to deep indoor. The angles of departure/arrival of the rays are obtained by applying a high resolution algorithm and values of the angular spread are given. Lastly, the maximum capacity of MIMO channels is presented both for co-and cross-polarization.

***Keywords*—**Indoor propagation, indoor penetration, polarization diversity, polarization diversity. MIMO

I. Introduction

With the ever-growing development of high data rate mobile communication, the characterization of signal penetration into buildings is of prime importance. Numerous measurement campaigns have thus been carried out, the objective of most of them being to study the additional propagation loss for estimation of indoor coverage. A classification of the indoor environment was proposed in [1] by defining different categories as: indoor light, indoor and deep indoor, according to the position of the room inside the building referred to the face of the building illuminated by the base station. Measured path loss at 780 MHz [2] and 1800 MHz [3] was compared to values predicted by the COST 231 model. This model is based on empirical formulas expressed, among other parameters, in terms of the number of internal walls and the through-wall propagation loss. The additional attenuation at 1.8 GHz in comparison to the results obtained at 900 MHz was outlined in [4], the authors also emphasizing the influence of the position of the building referred to the base station (BS), i.e. if the building is in the Line Of Sight (LOS) or not (NLOS) of the BS. A statistical approach made in the 0.8-8 GHz band in numerous office buildings and multistory car parks was proposed in [5].

This work was partly supported as a CISIT project.

I. Vin, D. P. Gaillot, P. Laly, M. Lienard and P. Degauque are with the University of Lille, IEMN Laboratory, TELICE group, Villeneuve d'Ascq, 59655 France, phone: 33 3 20 43 48 49; email: kyoko.vin@ed.univ-lille1.fr; {davy.gaillot, pierre.laly, martine.lienard, pierre.degauque@univ-lille1.fr}

J. M. Molina-Garcia-Pardo is with the Technical University of Cartagena, Information Technologies and Communication Dept., 30202 Spain (email: josemaria.molina@upct.es).

Nevertheless, the inaccuracy in a path loss prediction method based on the distance between the receiver and the penetration point such as a window, was discussed in [6]. To get a better insight on the influence of the walls, penetration loss and reflection coefficient were measured at 5.8 GHz for different types of wall as dry wall, wood, and for various polarizations [7]. The difference in attenuation due to materials used either in old or in new constructions is studied in [8] in the 800 MHz-18 GHz frequency band. Path loss is of course one of the main characteristics to determine the coverage in an indoor environment. Nevertheless, recent wireless systems include Multiple-Input Multiple-Output (MIMO) transmission schemes. In this case, directional channel characteristics as the Angle of Arrival (AoA), Angle of Departure (AoD), correlation between array elements, strongly influence the performances of the link.

For a vertical polarization VV, i.e. used both at the transmitter and at the receiver, the power of the multipath components (MPC) and the values of AoA/AoD were statistically studied in [9]. The role of the polarization and the value of the Cross Polarization Discrimination (XPD) was briefly presented in [10] but for a purely indoor or outdoor scenario.

The objective of this work is thus to study the influence of the polarization of the incident wave not only on the penetration loss but also on the delay spread, AoA and XPD in different rooms inside the building to cover scenarios from indoor light to deep indoor. The center frequency is 1.3 GHz.

After describing in Section II, the geometrical configuration of the building and the measurement setup, the distribution of path loss and XPD are studied in Section III depending on the polarization of the transmitter and on the position of Rx inside the building. Similarly, the distribution of the AoA in the various rooms is presented in Section IV, MIMO capacity being studied in Section V.

II. Measurement Setup and Antenna Configuration

A. Measurement Setup

The transmitting (Tx) and and receiving (Rx) antenna arrays were situated at the first floor of 2 buildings, 50 m apart. The Tx antenna was put at a window facing the other building in which the Rx array was placed. Successive scenarios were considered as shown in Fig. 1, the Rx array being nearly in the

ISBN: 978-1-61804-318-4

center of each room or in a corridor (Positions P6 and P7). P4 and P5 correspond to an "indoor light", the windows of the room being illuminated by the incident wave.

However the windows for the case P5 are partly shadowed by the leaves of a tree. Lastly, P1, P2 and P3 are related to deep indoor scenarios. In this office building, all rooms are entirely furnished.

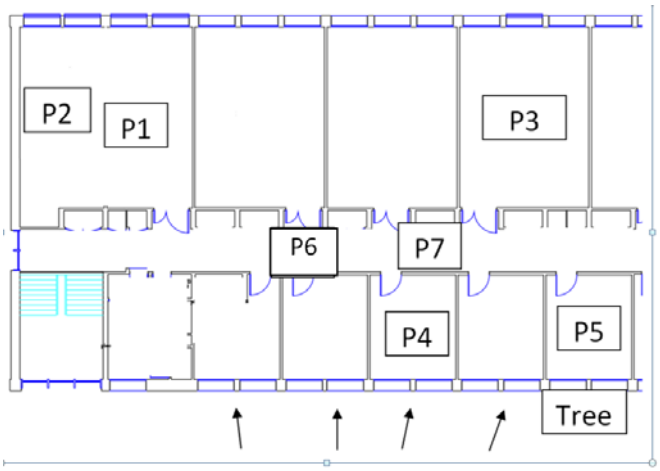

Fig. 1. Geometrical configuration of the measurement campaign. Successive positions of the Rx array are labeled P1 to P7.

The Tx antenna is a virtual 4-element uniform linear array (ULA), the element being a dual-polarized patch antenna whose center frequency is 1.3 GHz. Its orientation is such that the main lobe of its radiation pattern is directed towards the Rx building, the direction of the transmitting rays being given by the arrows in Fig. 1. At the receiving side, a 3x3 virtual uniform rectangular array (URA) is used, each element being also a dual-polarized patch antenna. The distance between the successive positions of the antenna is 10 cm, i.e. 0.43 λ, both for the ULA and the URA.

For each position, P1 to P7, the complex channel transfer functions H(f) between each element of the Tx and Rx arrays were measured with a vector network analyzer (VNA) on 512 equally spaced frequency points in a 22 MHz band with a center frequency of 1.3 GHz. The Rx antenna is directly connected to one port of the VNA using a low attenuation coaxial cable, 4 m long, a 30 dB low-noise amplifier being inserted or not, depending on the received power. Using a coaxial cable to connect the Tx antenna to the other port of the VNA leading to prohibitive attenuation, the signal of the Tx port of the VNA is converted to an optical signal sent through fiber optics, converted back to radio frequency and amplified. The phase stability of the fiber optics link has been checked and the calibration of the VNA takes amplifiers, cables, and optic coupler into account.

B. Radiation Pattern of the Antennas

One of the objective of the paper being to compare the channel characteristics for horizontal and vertical polarizations, it will be interesting to base this comparison on an Rx antenna presenting an omnidirectional radiation pattern, at least in the horizontal plane. Indeed, one can expect that the most powerful reflected rays will propagate inside the building with a small angle of elevation. To achieve this goal, the Rx patch antenna was rotated around its vertical axis, by steps of 90°. Summing the complex value of the field successively received for the 4 positions of the Rx antenna leads to a nearly omnidirectional pattern in the horizontal plane, as shown in Fig. 2, curve (a). This curve was obtained for an HH polarization, the first and the second letter referring to the polarization of the Tx and Rx antenna, respectively. As a comparison, the pattern of a single patch antenna is given by curve (b). A similar curve was obtained for VV.

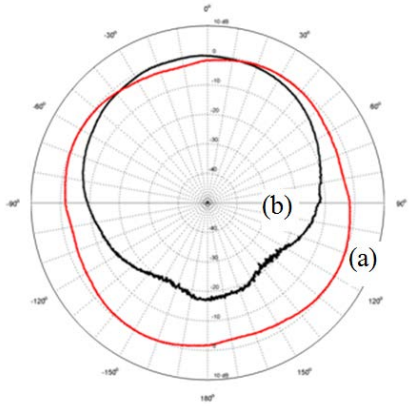

Fig. 2. Radiation pattern in the horizontal plane for HH polarization; (a) by summing the field radiated by the patch antenna in 4 orthogonal positions; (b) for a single patch antenna.

Lastly, to increase the signal-to-noise ratio (SNR), 10 successive measurements are averaged. The approach is thus rather long but, during the experiments, nobody was present in the building and the channel can be considered as stationary.

III. Path Loss and Cross Polarization Discrimination Factor from Indoor Light to Deep Indoor

A. Path loss

Let us first consider the variation of the signal amplitude when the receiver moves from P4 to P1 or P2. At P4, i.e. in indoor light conditions, the mean value of the received signal is maximum for an HH polarization (both Tx and Rx are horizontally polarized). Since we want to outline the additional attenuation from indoor light to deep indoor, this mean value is chosen as a reference (0 dB). Curves in Fig. 3 show the cumulative distribution function (cdf) of the relative loss for 4 possible combinations of the polarization.

This cdf was deduced from measurements made for the 9 positions of the Rx antenna (URA) at point P4, the 4 positions of Tx (ULA) and the 512 frequency points. For this scenario, waves remain polarized and HH is slightly better than VV.

Curves in Fig. 4 have been plotted for a deep indoor scenario (Position P1), the reference being always the mean value of the received signal HH in P4 (indoor light). The minimum loss is still obtained for co-polarized antennas, HH or VV. However, in this case, the waves are strongly depolarized; a cross polarization scenario (HV) presenting an attenuation less than 3 dB compared to HH.

ISBN: 978-1-61804-318-4

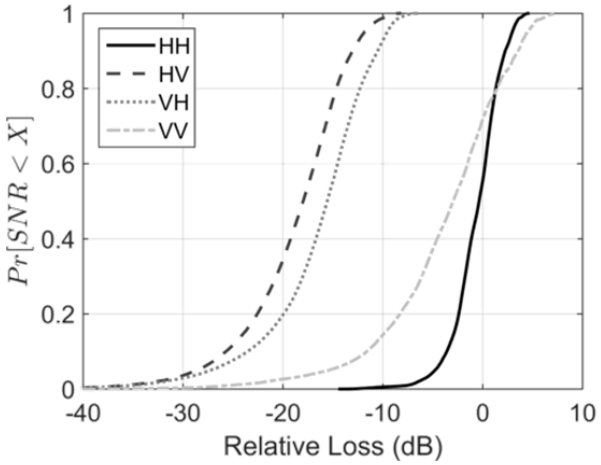

Fig. 3. Indoor light: cumulative distribution function of the additional loss referred to the mean value of the received signal for HH polarization.

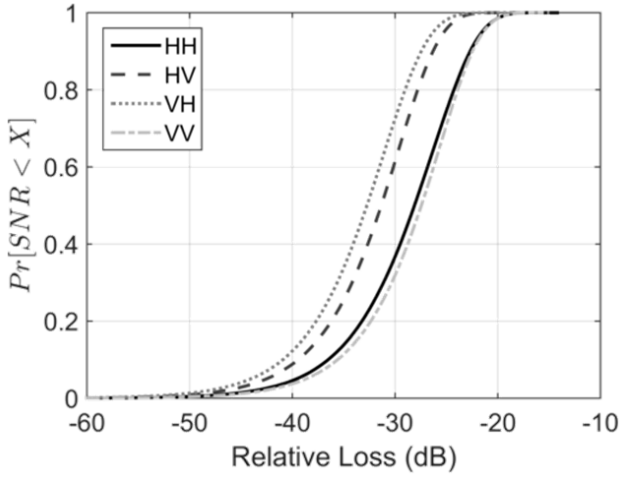

Fig. 4. Same as in Fig. 3 but for the deep indoor scenario P2.

Table I summarizes results obtained in the different scenarios. By choosing, as previously, the reference of 0 dB for "light indoor" and HH polarization, the mean additional path loss is given for co-polar and cross-polar configurations for: i) light indoor P4, ii) light indoor but in presence of a dense vegetation masking the line of sight ("Light obstructed" P5), iii) in the corridor (P6 and P7) and lastly iv) in deep indoor (P1, P2 and P3).

The averaging made over various positions inside the different rooms confirms the less important additional losses for co-polarization even in deep indoor. Furthermore, if we compare results for light indoor, obstructed or not by a tree with dense foliage, it appears that the presence of such a tree near a window increases the attenuation of 6 to 10 dB.

B. Delay Spread

Curves in Fig. 5 give the power delay profile (pdp) for a deep indoor scenario and for different polarizations. The shapes of the pdp for other scenario are similar and one can expect that the rms delay spread will have the same order of magnitude.

Table I. Mean additional path loss (in dB) for various receiving scenarios: Light indoor ("Light"); LOS obstructed ("Light. obst."), corridor and deep indoor.

	Light	Light obst.	Corridor	Deep
HH	0	-9	-12	-25
HV	-17	-18	-23	-30
VV	-1	-11	-12	-27
VH	-14	-19	-21	-30

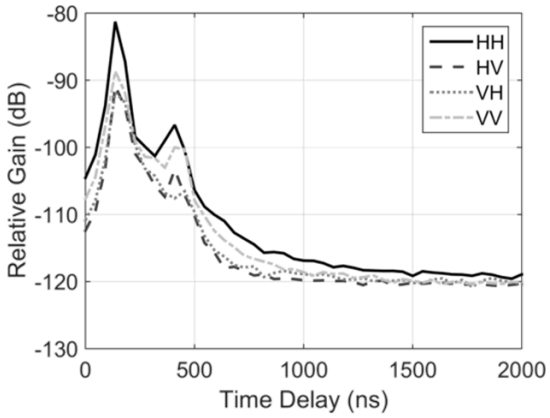

Fig. 5. Power delay profile for the deep indoor scenario P1.

This appears in Table II summarizing results obtained in the different scenarios, considering a threshold of -20 dB.

Table II. Mean rms delay spread (in ns) for the different scenarios

	Light	Light obst.	Corri.	Deep
HH	39	31	36	70
HV	39	36	41	108
VV	35	39	35	80
VH	32	37	34	100

As expected, the delay spread increases when the receiver moves from indoor light to deep indoor, varying from about 35-40 ns to 70-100 ns. Furthermore, the difference between co-and cross-polarization configurations is not important, except in deep indoor.

IV. Channel Characteristics Deduced from High Resolution Algorithm

Directional channel characteristics are deduced from the previous results by applying the RiMAX High Resolution Algorithm (HRA). It allows getting a joint estimation of the relative time of arrival (delay), the angle of arrival (AoA) and the angle of departure (AoD). It must be emphasized that the performance of an HRA is highly sensitive to the frequency band, to the number of frequency points in this band, and to the number of spatial samples corresponding to the number of array elements which is rather small in our application.

The presence of correlated paths (e.g. clusters) in the channel also strongly affects parameter estimation. In our case, the multipath components (MPC) were extracted from RiMAX by considering 351 frequency points in the 22 MHz

band, the 3x3 URA and the 4-ULA used for the Rx and Tx array, respectively. An example of the transmitting and receiving rays deduced from RiMAX is given in Fig. 6 where Rx is situated in position P2, i.e. in deep indoor for HH polarization. In this case, 15 rays having an attenuation less than 20 dB, referred to the most powerful ray, have been obtained. At Rx, a wide spread of the AoA is observed, this spread being much smaller at the Tx site, the antenna directly illuminating the Rx building.

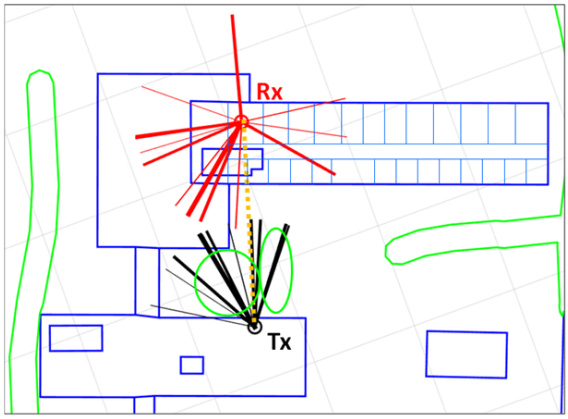

Fig. 6. Ray-tracing of the estimated paths for P2. The path thickness is proportional to the power.

Table III gives the rms angular spread of the AoA/AoD for the different positions of Rx in the building and, in each case, for the best polarization, i.e. presenting the lowest path loss.

Table III. Mean rms angular spread for the different scenarios

	Light	Light obst.	Corridor	Deep
AoA	12°	64°	40°	83°
AoD	12°	23°	20°	40°

V. MIMO CAPACITY WITH UNIFORM LINEAR ARRAY

For a MIMO transmission based on ULA, it is interesting to know if the orientation of the ULA inside the building has a great influence or not on the channel capacity. We will thus consider a (4,3) MIMO system as shown in Fig. 7.

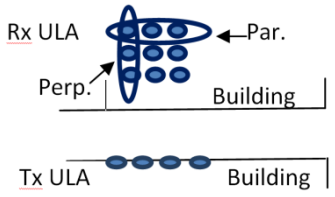

Fig. 7. Geometrical configuration of the simulated MIMO system.

The alignment of the Rx ULA is either parallel or perpendicular to the Tx ULA, and noted in Fig. 7 "Par.' and "Perp.", respectively. The channel capacity was calculated by assuming an SNR of 35 dB in room P4, for HH polarization and takes the additional losses into the rooms into account.

Let us recall that this position was chosen as a reference point in Section III, Table I. Results detailed in Table IV are related to the parallel configuration, but nearly the same results were obtained for the Rx ULA in the "perpendicular" orientation. The orientation of the ULA inside the room is thus not at all a critical parameter.

Table IV. Capacity (bits/s/Hz) for the different scenarios. "Parallel configuration".

	Light	Light obst.	Corri.	Deep
HH	33	27	24	16
HV	25	23	18	10
VV	37	31	27	13
VH	26	22	19	10

VI. CONCLUSION

We have shown that the cross-polar discrimination factor varies from 13-15 dB for indoor light to only few dBs for deep indoor. The rms delay spread, varies from 30 to 100 ns and is slightly higher for a cross-polar configuration, mainly for deep indoor. The angular spread at the receiver reaches 80° for deep indoor. Lastly, for a MIMO link using a linear array, the best results in terms of capacity were obtained for a co-polar configuration. Furthermore, the capacity is not strongly dependent on the orientation of the receiving array inside the building.

REFERENCES

[1] L. Ferreira, M. Kuipers, C. Rodrigues and L. M. Correia, "Characterisation of signal penetration into buildings for GSM and UMTS," in *Proc. Int. Symp. Wireless and Commun. Systems*," 2006, pp. 63-67.

[2] E. Suikkanen, A. Tölli and M. Latva-aho, "Characterization of propagation in an outdoor to indoor scenario at 780 MHz," in *Proc. 21st Int. Symp. on PIMRC*, 2010, pp. 70-74

[3] R. Visbrot, A. Kozinsky, A. Freedman, A. Reichman and T. Blaunstein, "Measurement campaign to determine and validate outdoor to indoor propagation models for GSM signals in various environments," in *Proc. IEEE Int. Conf. on COMCAS*, 2011, pp. 1-5

[4] D. M. Rose and T. Kurner, "Outdoor to indoor propagation – Accurate measuring and modeling of indoor environment at 900 and 1800 MHz," in *Proc. European Conf. Antennas and Propag. (EUCAP)*, 2012, pp. 1440-1444.

[5] H. Okamoto, K. Kitao and S. Ichitsubo, "Outdoor-to-indoor propagation loss prediction in 800 MHz to 8 GHz band for an urban area," *IEEE Trans. Vehicular Techno.*, vol. 3, pp. 1059-1067, March 2009.

[6] Y. Hirota, H. Izumikawa and C. Ono, "Outdoor-to-indoor radio propagation characteristics with 800 MHz band in an urban environment," in *Proc. IEEE Antennas Propagation/URSI Symp.*, 2014, pp. 697-698.

[7] Y. Azar, H. Zhao and M. E. Knox, "Polarization diversity measurements at 5.8 GHz for penetration loss and reflectivity of common building materials in an indoor environment," in *Proc. 3rd Int. Conf. Future Generation Commun. Techno,"* pp. 50-54, Aug. 2014

[8] I. Rodriguez, H. C. Nguyen, N. Jorgensen, T. Sorensen and P. Mogensen, "Radio propagation into modern buildings: Attenuation measurements in the range from 800 MHz to 18 GHz," in *Proc. 80th IEEE Vehicular Techno. Conf.*, 2014, pp. 1-5

[9] S. Wyne, A. F. Molisch, P. Almers, G. Eriksson, J. Kardeal and F. Tufvesson, "Outdoor to indoor MIMO measurements and analysis at 5.2 GHz," *IEEE Trans. Vehicular Techno.,"* vol. 57, pp. 1374-1386, May 2008

[10] E. M. Vitucci, F. Mani, C. Oestges and V. Degli-Esposti, "Analysis and modeling of the polarization characteristics of diffuse scattering in indoor and outdoor radio propagation", in *Proc. of Int. Conf. on applied EM and Commun.*, 2013, pp. 1-5

ISBN: 978-1-61804-318-4